American Mineralogist, Volume 97, pages 2049–2055, 2012

AMORPHOUS MATERIALS: PROPERTIES, STRUCTURE, AND DURABILITY†

First-principles study of self-diffusion and viscous flow in diopside ($CaMgSi_2O_6$) liquid

ASHOK K. VERMA[1] AND BIJAYA B. KARKI[2,*]

[1]High Pressure and Synchrotron Radiation Physics Division, Bhabha Atomic Research Centre, Mumbai 400085, India
[2]Department of Computer Science, Department of Geology and Geophysics, Center of Computation and Technology, Louisiana State University, Baton Rouge, Louisiana 70803, U.S.A.

ABSTRACT

We have carried out equilibrium molecular dynamics simulations of $CaMgSi_2O_6$ (diopside) liquid as a function of pressure (up to 150 GPa) and temperature (2200 to 6000 K) using density functional theory. Self-diffusion of Mg/Ca atoms decouples most from that of framework (Si/O) atoms at 2200 K and zero pressure, and all diffusivities become increasingly similar as temperature and pressure increase. The predicted temperature variations of all transport coefficients at zero pressure closely follow the Arrhenian law with activation energies of 107 to 161 kJ/mol. However, their pressure variations show significant deviations from the Arrhenius behavior. Along the 3000 K isotherm, the Si and O self-diffusivities show non-monotonic variations up to 20 GPa and then rapidly decrease upon further compression. The melt viscosity also shows a weak anomaly in the low-pressure regime before it starts to increase rapidly with pressure. Our results agree favorably with experimental observations of low-pressure non-uniform variations of Si and O self-diffusivities and viscosity. The predicted complex dynamical behavior requires pressure-volume dependent activation volumes and can be associated with structural changes occurring on compression.

Keywords: Diopside liquid, diffusion, viscosity, first-principles simulations, high pressure

INTRODUCTION

Knowledge about molten silicates is crucial for our understanding of the cooling and crystallization of Earth's early magma ocean as well as for our understanding of the magmatic processes at the present (e.g., Abe 1997; Solomatov 2007; Lee et al. 2010). The analysis of xenoliths (Haggerty and Sautter 1990) and seismic observations (Revenaugh and Sipkin 1994; Lay et al. 2004) suggest that melts can exist at various depths in the mantle including the core-mantle boundary and can have a broad range of composition. Despite their great geophysical and geochemical importance, experimental studies of relevant silicate melts are still limited to relatively low pressures and temperatures, particularly, in the case of transport properties. Recently, we have reported first-principles studies of self-diffusion and viscous flow for several key liquids including SiO_2 (Karki and Stixrude 2010a), Mg_2SiO_4 (Ghosh and Karki 2011), $MgSiO_3$ (Karki and Stixrude 2010b), and $CaAl_2Si_2O_8$ (Karki et al. 2011).

Here, we study the transport properties of diopside ($CaMgSi_2O_6$) liquid, which being an end-member of model basalt composition (0.64 diopside + 0.36 anorthite) and representing a tertiary (CaO-MgO-SiO_2) system is a key component of the most common magma (basaltic melt). Diopside liquid has a relatively depolymerized structure and is expected to show faster and simpler dynamics than highly polymerized liquids (e.g., Bottinga and Richet 1995). Experimental data on self-diffusion and viscosity coefficients of diopside liquid currently exist at temperatures below 2500 K and pressures below 15 GPa (Dunn 1982; Urbain et al. 1982; Scarfe et al. 1987; Shimizu and Kushiro 1991; Reid et al. 2001, 2003). The estimated activation energies and volumes of self-diffusion and viscous flow vary largely among these studies thereby rendering any extrapolations to high pressures uncertain. On the other hand, first-principles approach allows us to make reasonably accurate quantitative predictions of the values of these transport coefficients over much wider pressure and temperature ranges. In addition, the simulations are expected to provide insight into underlying microscopic mechanisms in the form of the atomic trajectories. In this endeavor, a recent study has addressed the structure and thermodynamics of diopside liquid (Sun et al. 2011). By performing equilibrium molecular dynamics simulations of molten $CaMgSi_2O_6$, we calculate here from first-principles its self-diffusion and viscosity coefficients as a function of pressure (up to ~150 GPa) and temperature (2200 to 6000 K).

The paper is organized as follows. First, we introduce the methodology in the context of simulations, and derivation and analysis of the dynamical properties. Then, we present the specific results and discussion on melt transport properties by comparing our predictions with relevant experimental and calculated results for other silicate melts.

METHODOLOGY

First-principles molecular dynamics method (Kresse and Furthmuller 1996) was used within the local density approximation (LDA). The projector augmented wave (PAW) method (Kresse and Joubert 1999) was used with a plane wave cutoff of 400 eV and γ point. Simulations (consisting of 80 and 160 atoms) based on the canonical (*NVT*) ensemble were performed to explore compression from $V/V_X = 1.5$ to 0.45 covering pressure range of 0 to 150 GPa at 2200 to 6000 K, where $V_X = 81.8$ cm^3/mol is the reference volume also used in the previous study (Sun et al. 2011). The initial structure at each volume was first melted at 6000 K and then cooled isochorically to lower temperatures. Long simulation durations ranging from 20 to

* E-mail: karki@csc.lsu.edu

† Information about the Amorphous Materials special section papers can be found on GSW at http://ammin.geoscienceworld.org/site/misc/virtual_special_list.xhtml. Additionally the GSW site has a classification tag found on the right that is a link to all the papers. The MSA website also has special section information.

0003-004X/12/1112–2049$05.00/DOI: http://dx.doi.org/10.2138/am.2012.4123

500 ps with time step (1 fs) were performed to achieve an acceptable convergence for dynamical properties being studied. We confirm the liquid state of the simulated system at each *V*-*T* condition by examining the radial distribution functions and mean-square displacements. The uncertainties in the pressure and energy computed using the blocking method (Flyvbjerg and Petersen 1989) are limited within ±0.5 GPa and ±0.2 eV/formula, respectively. The Pulay stress arising from the finite plane wave basis set used varies nearly linearly from 2 to 7 GPa over the volume range studied. An empirical correction of 2.5 GPa to the total pressure to account for the overbinding effects of LDA was applied at each volume (de Koker et al. 2008; Sun et al. 2011).

We compute the self-diffusion coefficient for each species α from first-principles equilibrium molecular dynamics simulations using the Einstein relation

$$D_\alpha = \lim_{t\to\infty} \frac{1}{6t} \left\langle \frac{1}{N_\alpha} \sum_{i=1}^{N_\alpha} \left| \vec{r}_{\alpha,i}(t+t_0) - \vec{r}_{\alpha,i}(t_0) \right|^2 \right\rangle . \quad (1)$$

The positions of the i^{th} atom of type α at time origin t_0 and then after time t are $\vec{r}_{\alpha,i}(t_0)$ and $\vec{r}_{\alpha,i}(t+t_0)$, respectively. We calculate the shear viscosity (η) using the Green-Kubo relation

$$\eta = \frac{V}{10 k_B T} \int_0^\infty \left\langle \sum_{\alpha\beta} w_{\alpha\beta} P_{\alpha\beta}(t+t_0) \cdot P_{\alpha\beta}(t_0) \right\rangle dt . \quad (2)$$

Here, the deviatoric stress tensor $P_{\alpha\beta}$, which is the symmetrized traceless portion of the stress tensor computed at every FPMD step, and $w_{\alpha\beta}$ is 4/3 and 1 for diagonal and off-diagonal components, respectively. Further details can be found in our previous studies (Karki et al. 2011; Ghosh and Karki 2011).

Simulation Results

First, we briefly present the calculated pressure-volume-temperature results, which can be accurately represented by the third-order Birch-Murnaghan equation of state (EOS) for the reference isotherm, $P(V,T_0)$, and a simple form of the thermal pressure, $P_{TH}(V,T) = B(V)(T - T_0)$. The 3000 K reference EOS parameters are: V_0 = 95 (±2) cm^3/mol, K_0 = 13.2 (±5) GPa, and K_0' = 5.4 (±6), and the thermal pressure coefficient is: $B(V) = 27.4 - 0.54V + 0.00278V^2$ in MPa/K. The results agree well with a recent first-principles study (Sun et al. 2011). This means that the use of larger supercell size, longer simulation runs, and PAW potentials does not have significant effects on the predicted melt structure and thermodynamics.

Self-Diffusion Coefficients

Self-diffusion coefficients of all four species (Ca, Mg, Si, and O) at zero pressure were calculated at seven temperatures from 2200 to 6000 K (Fig. 1a). At the lowest temperature studied, Ca, and Mg are much more mobile than Si and O, with Ca being the fastest species and Si being the slowest species. With increasing temperature over this range, the Ca and Mg diffusivities increase much less (by a factor of ~40 to ~55) compared to Si diffusivity, which increases by a factor of ~240. The O diffusivity shows an intermediate level of variation (~150-fold increase) with temperature. Our results thus show that with decreasing temperature, the movements of different species decouple more and more from each other. The framework (Si/O) atoms can be viewed as frozen with respect to the timescale of motion of Mg/Ca atoms at the lowest temperature of 2200 K. Despite substantial differences in the extents of temperature variations, the calculated self-diffusion coefficients of all species closely follow the Arrhenian relation: $D_\alpha = D_{0\alpha} \exp[-E_\alpha/(RT)]$, where α represents atomic species. The activation energies fall in the range 107 to 161 kJ/mol (Table 1)

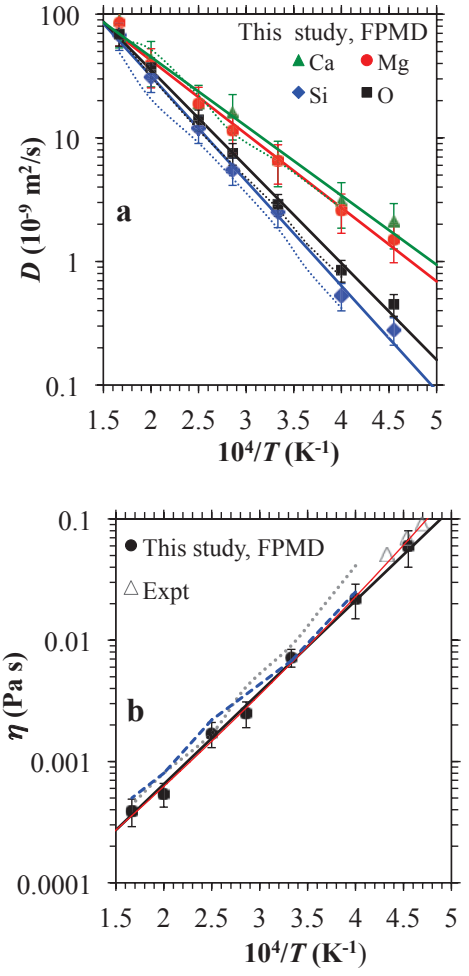

Figure 1. Calculated self-diffusivities of different species (**a**) and viscosity (**b**) of diopside liquid as a function of temperature at zero pressure (±1 GPa). The straight solid lines are the Arrhenian representations of the calculated data. The experimental viscosity data (triangles) are from Urbain et al. (1982). Also shown are previous first-principles results (dotted lines) of anorthite liquid (Karki et al. 2011) and only viscosity results (dashed lines) of enstatite liquid (Karki and Stixrude 2010b). The VFT viscosity fit is shown by thin (red) line. (Color online.)

in the $E_{Ca} < E_{Mg} < E_O < E_{Si}$ order. They are generally smaller than the values derived from low temperature (<2500 K) experimental data for diopside liquid. The experimentally derived activation energies for various silicate liquids vary from ~180 to ~270 kJ/mol for Si and O diffusion (Dunn 1982; Shimizu and Kushiro 1991; Reid et al. 2001; Tinker et al. 2003).

The calculated self-diffusivities of different species in diopside liquid vary with pressure in a way that is sensitive to temperature (Fig. 2). At 6000 and 4000 K, all diffusivities show a normal trend in that they decrease monotonically with pressure. The Ca and Mg diffusivities decrease with pressure more rapidly at lower temperatures. However, both framework ions (Si and O) at 3000 K show a different behavior in the low-pressure regime (below 20 GPa). Their diffusivities tend to initially remain unchanged or even increase somewhat with pressure before they start decreasing rapidly and monotonically on further compression, i.e.,

TABLE 1. Arrhenius fit parameters for the temperature variations of the self-diffusion and viscosity coefficients at zero pressure (±1 GPa) of the simulated diopside liquid

Parameters	D_{Ca}	D_{Mg}	D_{Si}	D_O	η
D_0 (10^{-9} m^2/s), η_0 (Pa s)	597	652	1540	1275	0.000018
Anorthite*	710	–	1290	1450	0.000015
Enstatite†	–	473	973	1314	0.000031
E_D or E_η (kJ/mol)	107 (7)	114 (5)	161 (5)	149 (4)	148 (5)
Anorthite*	117 (8)	–	166 (6)	158 (4)	162 (13)
Enstatite†	–	105 (5)	154 (9)	151 (10)	138 (7)
Expt	172		180‡, 267§	267§	155‖

Notes: The activation energies from previous calculations and experiments (specific reference footnoted) for diposide liquid are shown for comparisons. The experimental value for Ca diffusion is for hyplobasaltic melt (La Tourrette et al. 1996).
* Karki et al. (2011).
† Karki and Stixrude (2010b); Ghosh and Karki (2011).
‡ Shimizu and Kushiro (1991).
§ Reid et al. (2001).
‖ Urbain et al. (1982).

normal diffusion appears only in the high-pressure regime. Such non-monotonic (anomalous) pressure behavior is also present at the lowest temperature of 2500 K in narrow pressure range of 0–12 GPa studied here. Our predictions qualitatively agree with the experimental data of diopside liquid at temperatures below 2500 K and pressures up to 15 GPa (Reid et al. 2001) in the sense that the predicted and measured Si and O diffusivities do vary non-monotonically with pressure in the low-pressure regime. However, the experimental variations are stronger and show a trend that is opposite to calculated variations. The reason for this discrepancy is not clear. It is relevant here to point out that such non-monotonic changes in the pressure behavior of Si and O self-diffusion were previously predicted for other silicate liquids (e.g., Spera et al. 2009; Ghosh and Karki 2011; Karki et al. 2011) with anomalous behavior (increasing diffusivity on compression) being most pronounced in silica liquid (Karki and

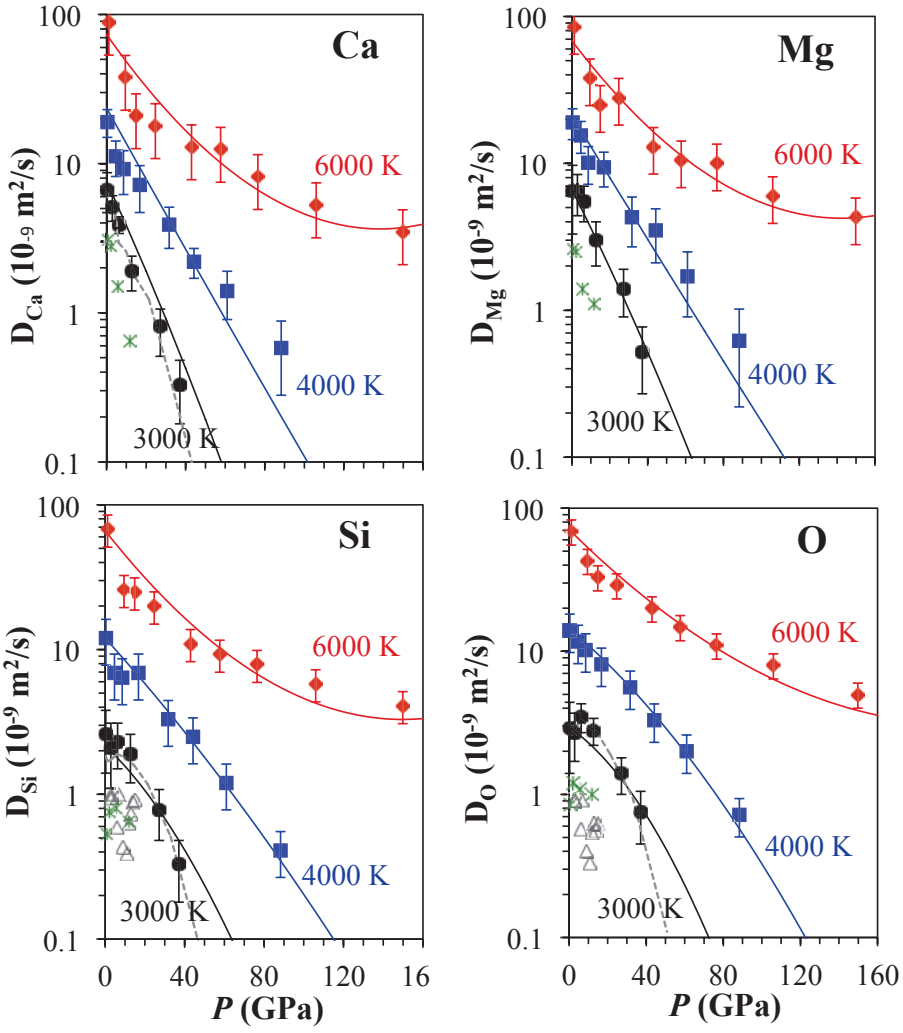

FIGURE 2. Calculated self-diffusion coefficients of Ca, Mg, Si, and O in diopside liquid as a function of pressure at 2500 K (asterisks), 3000 K (circles), 4000 K (squares), and 6000 K (diamonds). The lines are fit to the modified Arrhenius relation (Eq. 3). The experimental data for Si and O self-diffusion in diopside liquid over temperature range of 2073 to 2573 K at low pressures (shown by triangles) are from Reid et al. 2001. The gray dotted lines are the previous calculations at 3000 K for anorthite liquid (Karki et al. 2011). (Color online.)

Stixrude 2010a). As pointed out earlier, the predicted activation energies of self-diffusion are smaller than the experimentally derived values. Generally, the temperature and pressure ranges considered in the experiments are much narrower than those in the simulations thereby making the estimation of these parameters uncertain. More studies are needed to explain the noted dynamical differences among computations and experiments for diopside and other silicate liquids.

All three isotherms for the diffusivity of each species plotted in the logarithmic scale (i.e., $\log D_\alpha$) in Figure 2 are not straight lines suggesting that diffusivity does not vary with pressure according to the standard Arrhenian law. We represent the predicted complex pressure variation of self-diffusion coefficient for each species α using the modified Arrhenian relation (Nevins et al. 2009; Ghosh and Karki 2011):

$$D_\alpha(P,T) = D_{0,\alpha} \exp\left[\frac{E_\alpha + PV_\alpha(P,T)}{RT}\right]. \quad (3)$$

This means that the activation volume is a function of pressure and temperature:

$$V_\alpha(P,T) = (V_0 + V_1 T) + P(V_2 + V_3 T + V_4 / T) \quad (4)$$

where the fit parameters represent the pressure, temperature, and cross-derivatives of the activation volumes (Table 2). We adopt the values of the pre-exponential and activation energies from the zero pressure Arrhenian fitting given in Table 1. The low-pressure diffusion regime along 3000 K (and 2500 K) corresponds to almost zero activation volumes for Si and O but large positive volumes for Ca and Mg. As pressure rises, all activation volumes increase at 3000 K, remain nearly constant at 4000 K and decrease at 6000 K. These changes are significant in that the diffusivity isotherms show change in their curvatures—from concave to convex between 3000 and 6000 K. Such changes turn out to be the robust features also predicted in other silicate liquids as well (Karki and Stixrude 2010a, 2010b; Karki et al. 2011; Ghosh and Karki 2011).

Viscosity

The calculated viscosity increases with decreasing temperature at zero pressure by a factor of 130 over the temperature range (6000 to 2200 K) studied (Fig. 1b). The Arrhenian representation $\{\eta = \eta_0 \exp[E_\eta/(RT)]\}$ of viscosity gives the activation energy of 145 kJ/mol, which compares well with the experimentally derived value (~155 kJ/mol) for diopside liquid (Urbain et al. 1982, Scarfe et al. 1987) as shown in Table 1. The activation energy of viscous flow is thus intermediate between the activation energies of Si and O self-diffusion and those of Ca and Mg self-diffusion. This suggests that the motion of all atomic species is perhaps relevant for viscous flow. One possible mechanism is that as Ca/Mg atom diffuses through the melt, it drags the local disruption of the tetrahedral network along by activating BO↔NBO reaction. Note that the diopside liquid contains ~35% BO (bridging oxygen), ~64% (non-bridging oxygen), and ~1% oxygen not bonded to silicon at 3000 K and 0 GPa (with 92% Si-O tetrahedra). This process thus involves a local rearrangement of Si and O atoms, which facilitates not only Si and O diffusion but also eases viscous flow. It is remarkable that low-temperature extrapolation of our results slightly lies below the experimental data (Urbain et al. 1982). The measured and calculated data can be reconciled by assuming that the activation energy is a function of temperature, changing from a somewhat high value obtained from low-temperature measurements to a low value obtained from high temperature simulations. The Vogel-Fulcher-Tammann (VFT) formulation $\{\eta = A\exp[B/(T - T_0)]\}$, with A = 0.000028 Pa s, B = 14600 K, and T_0 = 300 K, permits the activation energy to vary with temperature over a wide range in a way that is seen in other silicate melts (Fig. 1b).

Like in the case of the diffusion, the pressure variation of the viscosity is sensitive to temperature and the logη curves are not straight lines (Fig. 3). We represent the predicted complex P-T behavior by the modified Arrhenian relation

$$\eta(P,T) = \eta_0 \exp\left[\frac{E_\eta / PV_\eta(P,T)}{RT}\right] \quad (5)$$

where the activation volume, $V_\eta(P,T)$, has the same form as Equation 4. The fit parameters are given in Table 1 and 2. The 6000

Table 2. Activation volumes and their pressure and temperature derivatives from the modified-Arrhenius representations (Eqs. 3 and 5) of the calculated self-diffusion and viscosity coefficients of diopside liquid

Parameters	V_0 cm³/mol	V_1 cm³/(mol·K)	V_2 cm³/(mol·GPa)	V_3 cm³/(mol·K·GPa)	V_4 cm³/(mol·K·GPa)
D_{Ca}	1.16	0.00017	0.0133	-3.6×10^{-6}	2.7
D_{Mg}	1.00	0.00016	0.0116	-3.1×10^{-6}	2.3
D_{Si}	−0.50	0.00042	0.0092	-3.3×10^{-6}	24
D_O	−0.47	0.00033	0.0010	-2.9×10^{-6}	23
η	−0.21	0.00050	0.0146	-4.6×10^{-6}	22

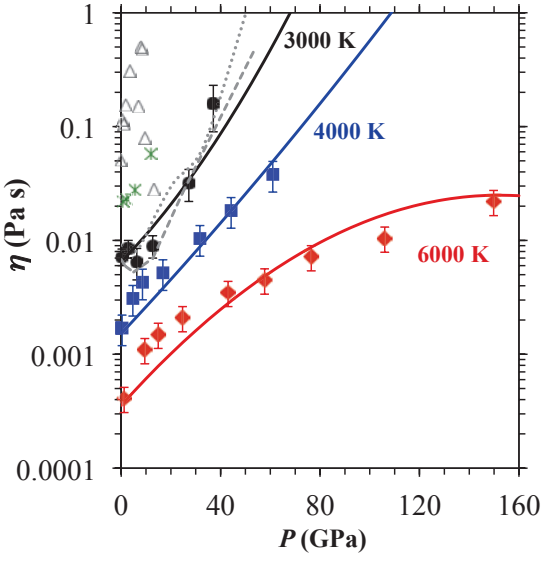

Figure 3. Pressure variations of the viscosity (solid symbols) of diopside liquid at 2500 K (asterisks), 3000 K (circles), 4000 K (squares), and 6000 K (diamonds) fit to the modified Arrhenian relation (Eq. 5). The gray dotted and dashed lines show the previous first-principle results at 3000 K for anorthite (Karki et al. 2011) and enstatite liquids, respectively. Various experimental data for the diopside liquid in the temperature range of 2000 to 2470 K at low pressures are also shown by triangles for comparison (Reid et al. 2003, and references therein). (Color online.)

and 4000 K isotherms show a clear normal trend of monotonically increasing viscosity with increasing pressure. However, the 2500 and 3000 K isotherms show a weak anomalous behavior in a narrow low-pressure regime before the viscosity (at 3000 K) increases rapidly and monotonically at pressures above 20 GPa. The viscosity isotherm thus changes from a convex curve to a concave curve between 3000 and 6000 K, which is opposite to the case of the diffusion. The other liquids were predicted to show a similar pressure-temperature behavior including the viscosity anomaly at 3000 K (Karki and Stixrude 2010a, 2010b). Our predicted behavior is consistent with the experimental observations of non-monotonic variation of viscosity with pressure up to 15 GPa (Reid et al. 2003) at temperatures lower than 2500 K. However, as in the case of Si and O self-diffusion, the experimentally measured pressure variations of the melt viscosity tend to show an opposite trend than the predicted variations.

Discussion

Our first-principles study suggests that Ca and Mg (network modifiers) diffuse much faster than Si and O (network formers) at low pressures and low temperatures, the differences in the diffusion between them being the largest at 2200 K and 0 GPa. Very similar diffusivities (within a factor of 1.3) at 6000 K suggest that the mechanisms for all species are similar at high temperatures in that they involve flow-like motion of particles mediated by frequent bond breakings. Table 3 shows the calculated rates (α_B) of bond events (bond breakages and formations) for all cation-anion bonds and also the estimated fractions (α_T) of these bond events that result in the formation of new bonds as opposed to the formation of the same bonds (i.e., recombination), which are just broken. This process of new bond formation causes the transfer of oxygen atom from one coordination shell to another thereby significantly contributing to the dynamics. Such bond events are prevalent at high temperatures as shown by high α_T values (Table 3) for each cation-anion bond type. As temperature decreases, the mechanisms become increasingly sensitive to local structural environments and different cation species see different local potentials. In particular, Si atom sits in a deeper minimum and its diffusion motion is not simply related to the breakage of the strong bond with one of its O neighbors. On the other hand, Ca, and Mg atoms being weakly bonded to O atoms can move easily in open space available at large volumes. The Ca/Mg-O bonds are much larger than the Si-O bonds (Fig. 4) and broken at much higher rates (Table 3).

Diffusivity differences among different species are suppressed on compression. Along 3000 K, the D_{Ca}/D_O, D_{Mg}/D_O, and D_{Si}/D_O ratios are 2.4, 2.2, and 0.9, respectively, at zero pressure, and 0.45, 0.69, and 0.44, respectively, at 37 GPa. Whereas the cation Ca is the fastest species at low pressure, the anion O is the fastest species at high pressure. Pressure-induced slowing down of Ca/Mg can be associated with the enhanced local structure consisting of Ca/Mg and O atoms on compression. The first peak in the calculated Ca-O and Mg-O radial distribution functions (RDF) become sharper closely resembling the Si-O peak as the liquid is compressed (Fig. 4). Following an initial relatively rapid increase, both Ca-O and Mg-O coordination tends to saturate at high pressures where the corresponding cation-anion bond-lengths rapidly decrease (Sun et al. 2011). On the other hand, the average Si-O bond-length initially increases with pressure over a wider range and then decreases at high pressure. The Si-O coordination changes from a tetrahedral environment at zero pressure to an octahedral environment with the preponderance of fivefold states at pressures around 20 GPa (Sun et al. 2011). Pressure thus suppresses the difference in the strength and breaking rates between Ca/Mg-O and Si-O bonds (Table 3). All cations see similar local environments and are equally trapped in the polyhedral cages and as such, they become systematically slower than the anion with their diffusion coefficients becoming comparable with each other.

We compare the predicted results of the diopside liquid with previous calculations on enstatite liquid (Karki and Stixrude 2010b) and anorthite liquid (Karki et al. 2011) to examine the effects of CaO and Al_2O_3 components on the transport properties. The self-diffusion (Si and O) and viscosity coefficients of the

Table 3. Calculated Ca-O, Mg-O, and Si-O bond related parameters at different conditions: α_B is the rate of bond-breakings (per picosecond) and α_T represents the fraction of the bond events that form new bonds

T (K), P (GPa)	Ca-O		Mg-O		Si-O	
	α_B	α_T	α_B	α_T	α_B	α_T
2500, 0.6	636	0.13	408	0.17	44	0.45
3000, 0.4	672	0.15	464	0.19	88	0.56
6000, 1.0	888	0.28	748	0.32	576	0.55
3000, 37	952	0.04	816	0.05	464	0.09

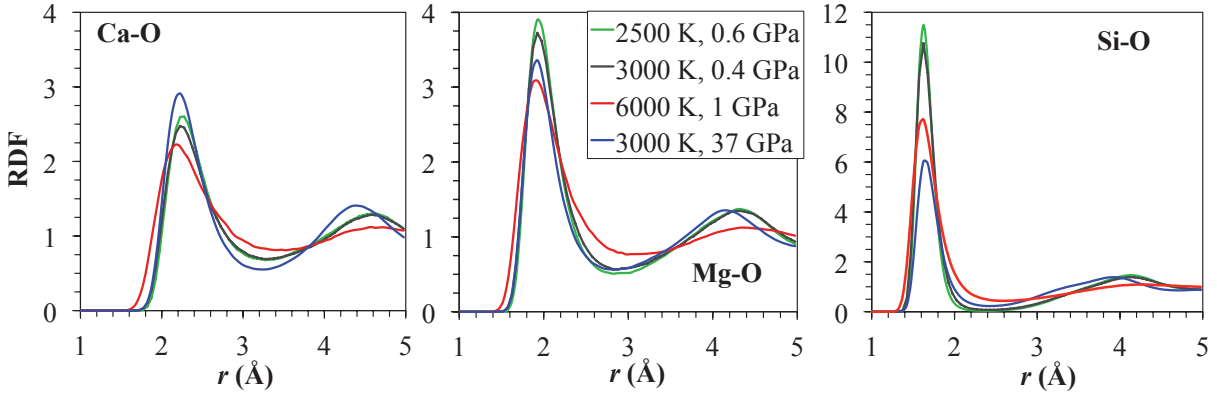

Figure 4. Ca-O, Mg-O, and Si-O radial distribution functions (RDF) of the simulated diopside liquid at different conditions as shown in the middle plot. (Color online.)

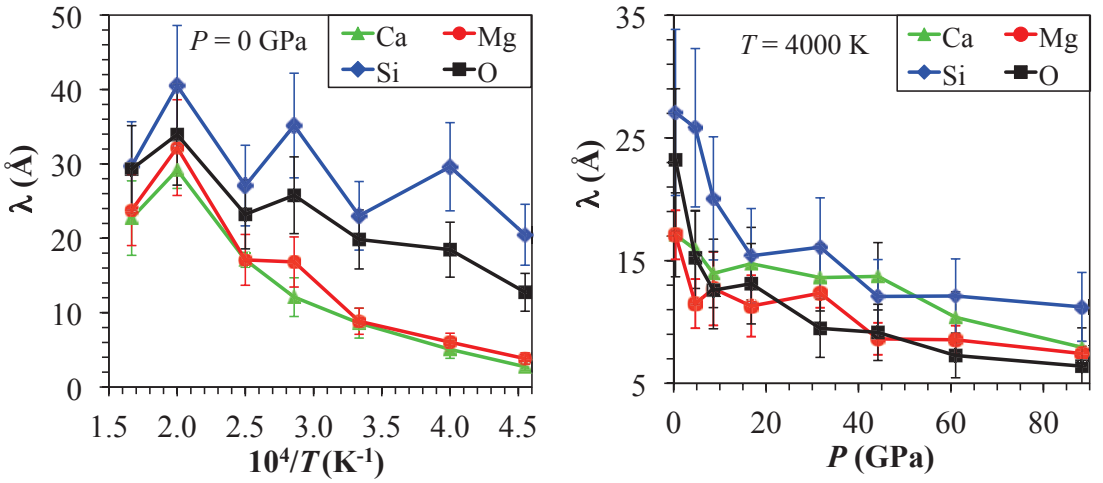

FIGURE 5. Estimated characteristic length (λ) as a function of temperature (2200 to 6000 K) at the zero pressure (**left**) and as a function of pressure at 4000 K (**right**) for different atomic species as shown. (Color online.)

diopside liquid are systematically larger and smaller, respectively, than those of the anorthite liquid at zero pressure (Figs. 1a and 1b) and elevated pressures (Figs. 2 and 3). Also, the diopside liquid tends to have smaller activation energies (Table 1) and weaker low-pressure dynamical anomalies than the anorthite liquid does. This is consistent with the structural difference between two liquids in terms of the degree of polymerization. Our first-principles study thus confirms that the diopside liquid with a relatively more depolymerized structure shows faster dynamics than the anorthite liquid. On the other hand, the diopside and enstatite liquids show similar dynamical behavior (Figs. 1b and 3) suggesting no discernable differences in the role of the CaO and MgO components. It is remarkable that the predicted differences in the transport coefficients between the diopside liquid studied here and anorthite liquid studied previously (Karki et al. 2011) are not substantial over the entire pressure-temperature conditions studied. This means that the first-principles results can provide useful constraints on the transport properties of the $CaMgSi_2O_6$-$CaAl_2Si_2O_6$ system, which represents a compositional analog for basaltic melt. In particular, the viscosity of major magma-forming silicate melts is expected to remain approximately unchanged with pressure over shallow depth range (up to ~20 GPa) of the mantle.

The widely used relation between the self-diffusion and viscous flow has the following form

$$\frac{k_B T}{\eta D_\alpha} = \lambda_\alpha \qquad (6)$$

where λ_α is a constant (for species α) and can have different meanings. According to the Stokes-Einstein formulation, the constant is related to the radius or size (a_α) of diffusing unit in the liquid (e.g., $\lambda_\alpha = 4\pi a_\alpha$). On the other hand, Eyring theory interprets it as an elementary diffusion step, i.e., a translation or jump distance of the diffusing ion. Previous studies have reported some success of the above relationship (Eq. 6) for silicate liquids with a jump distance (λ_0) equal to 2.8 Å for oxygen ion in estimating one transport property if the other is known (Poe et al. 1997; Reid et al. 2001, 2003; Mungall 2002; Tinker et al. 2004). Our first-principles diffusivity and viscosity results representing independent calculations can be used to evaluate the validity of Equation 6 over broad ranges of temperature and pressure. We find that λ_α for each species is a function of both temperature and pressure (Fig. 5). At zero pressure, all λ_α values tend to increase and converge with increasing temperature. There is also a clear separation between the λ_α values of framework (Si and O) and non-framework (Ca and Mg) ions as expected because of their different diffusivity-temperature behavior. For oxygen diffusion, λ_0 varies between 18 and 34 Å over the temperature range studied at zero pressure, which are much larger than the usually adopted jump distance of 2.8 Å for the diffusing O ion in silicate liquids. These λ_0 values correspond to a range of 1.5–2.7 Å for the radius of the diffusing O ion, compared to its actual radius of 1.4 Å. The estimated sizes of Ca and Mg ions lie between 0.4 and 2.6 Å, the actual radii being 1.14 and 0.86 Å, respectively. The estimated size of Si ion ranges from 1.8 to 3.2 Å, which are much larger than the actual radius of 0.54 Å. Though all λ_α values decrease with increasing pressure, their values at high pressure are still too large (for instance, 6.8 to 11.2 Å at 88 GPa and 4000 K) to be interpreted as the ionic translation distances. Also, the estimated sizes of diffusing species are either underestimated or overestimated relative to their actual radii. Such inconsistencies have previously been noted for silicate liquids based on computations (Lacks et al. 2007; Spera et al. 2009; Nevins et al. 2009; Ghosh and Karki 2011) as well as experiments (Mungall 2002; Reid et al. 2003; Tinker et al. 2004). This means that the diffusion of individual ions through the liquid may not alone control viscous flow. One can adopt an alternative interpretation such as one relating λ_α to the size of activated complexes or regions consisting of several atoms (e.g., Spera et al. 2009; Lesher 2010). As suggested earlier, the diffusion of Ca/Mg atoms facilitates the diffusion of Si and O, and these atomic movements together can be responsible for stress relaxations in the silicate melt. (Supplementary information is available[1].)

[1] Deposit item AM-12-090, supplementary information. Deposit items are available two ways: For a paper copy contact the Business Office of the Mineralogical Society of America (see inside front cover of recent issue) for price information. For an electronic copy visit the MSA web site at http://www.minsocam.org, go to the *American Mineralogist* Contents, find the table of contents for the specific volume/issue wanted, and then click on the deposit link there.

ACKNOWLEDGMENTS

This work was supported by NSF (EAR-1118869). High-performance computational resources were provided by Louisiana State University and Bhabha Atomic Research Center.

REFERENCES CITED

Abe, Y. (1997) Thermal and chemical evolution of the terrestrial magma ocean. Physics of Earth and Planetary Interiors, 100, 27–39.

Bottinga, Y. and Richet, P. (1995) Silicate melts: The anomalous pressure dependence of the viscosity. Geochimica et Cosmochimica Acta, 59, 2725–2731.

de Koker, N., Stixrude, L., and Karki, B.B. (2008) Thermodynamics, structure, dynamics, and melting of Mg_2SiO_4 liquid at high pressure. Geochimica et Cosmochimica Acta, 72, 1427–1441.

Dunn, T. (1982) Oxygen diffusion in three silicate melts along the join diopside-anorthite. Geochimica et Cosmochimica Acta, 46, 2293–2299.

Flyvbjerg, H. and Petersen, H.G. (1989) Error estimates on averages of correlated data. Journal of Chemical Physics, 91, 461–466.

Haggerty, S.E. and Sautter, V. (1990) Ultradeep (greater than 300 kilometers), ultramafic upper mantle xenoliths. Science, 248, 993–996.

Ghosh, D.B. and Karki, B.B. (2011) Diffusion and viscosity of Mg_2SiO_4 liquid at high pressure from first principles simulations. Geochimica et Cosmochimica Acta, 75, 4591–4600.

Karki, B.B. and Stixrude, L. (2010a) First-principles study of enhancement of transport properties of silica melt by water. Physical Review Letters, 104, 215901.

——— (2010b) Viscosity of $MgSiO_3$ liquid at Earth's mantle conditions: Implications for an early magma ocean. Science, 328, 740–743.

Karki, B.B., Bohara, B., and Stixrude, L. (2011) First-principles study of diffusion and viscosity of anorthite ($CaAl_2Si_2O_8$) liquid at high pressure. American Mineralogist, 96, 744–751.

Kresse, G. and Furthmuller, J. (1996) Efficiency of ab-initio total energy calculations for metals and semiconductors using a plane-wave basis set. Computational Materials Science, 6, 15–50.

Kresse, G. and Joubert, D. (1999) From ultrasoft pseudopotentials to the projector augmented-wave method. Physical Review B, 59, 1758–1775.

La Tourrette, T., Wasserburg, G.J., and Fahey, A.J. (1996) Self diffusion of Mg, Ca, Ba, Nd, Yb, Ti, Zr, and U in haplobasaltic melt. Geochimica et Cosmochimica Acta, 71, 1312–1323.

Lacks, D.J., Rear, D., and Van Orman, J.A. (2007) Molecular dynamics investigation of viscosity, chemical diffusivities and partial molar volumes along the MgO-SiO_2 join as functions of pressure. Geochimica et Cosmochimica Acta, 71, 1312.

Lay, T., Garnero, E.J., and Williams, Q. (2004) Partial melting in a thermo-chemical boundary at the base of the mantle. Physics of Earth and Planetary Interiors, 146, 441–467.

Lee, C.A., Luffi, P., Hoink, T., Dasgupta, R., and Hernlund, J. (2010) Upside-down differentiation and generation of a primordial lower mantle, Nature, 463, 930–933.

Lesher, C.E. (2010) Self-diffusion in silicate melts: Theory, observations, and applications to magmatic systems. In Y. Zhang and D.J. Cherniak, Eds., Diffusion in Minerals and Melts, 72, p. 269–309. Reviews in Mineralogy and Geochemistry, Mineralogical Society of America, Chantilly, Virginia.

Mungall, J.E. (2002) Empirical models relating viscosity and tracer diffusion in magmatic silicate melts, Geochimica et Cosmochimica Acta, 66, 125–143.

Nevins, D., Spera, F.J., and Ghiorso, M.S. (2009) Shear viscosity and diffusion in liquid $MgSiO_3$: Transport properties and implications for terrestrial planet magma oceans. American Mineralogist, 94, 975–9801.

Poe, B.T., McMillan, P.F., Rubie, D.C., Chakraborty, S., Yarger, J., and Diefenbacher, J. (1997) Silicon and oxygen self diffusivities in silicate liquids measured to 15 gigapascals and 2800 Kelvin. Science, 276, 1245–1248.

Reid, J.E., Poe, B.T., Rubie, D.C., Zotov, N., and Wiedenbeck, M. (2001) The self-diffusion of silicon and oxygen in diopside ($CaMgSi_2O_6$) liquid up to 15 GPa. Chemical Geology, 174, 77–86.

Reid, J.E., Suzuki, A., Funakoshi, K.-I., Terasaki, H., Poe, B.T., Rubie, D.C., and Ohtani, E. (2003) The viscosity of $CaMgSi_2O_6$ liquid at pressures up to 13 GPa. Physics of Earth and Planetary Interiors, 139, 45–54.

Revenaugh, J. and Sipkin, S.A. (1994) Seismic evidence for silicate melt atop the 410-km mantle discontinuity. Nature, 369, 474–476.

Scarfe, C.M., Mysen, B.O., and Virgo, D. (1987) Pressure dependence of the viscosity of silicate melts. In: Mysen, B.O. (Ed.) Magmatic Processes: Physiochemical Principles, The Geochemical Society.

Shimizu, N. and Kushiro, I. (1991) The mobility of Mg, Ca, and Si in diopside-jadite liquids at high pressures. In Perchuk, L.L. and Kushiro, I., Eds., Physical Chemistry of Magmas. Springer-Verlag, Berlin

Solomatov, V.S. (2007) Magma oceans and primordial mantle differentiation in Treatise on Geophysics, vol. 9, p. 91, edited by G. Schudbert, Elsevier.

Spera, F.J., Nevins, D., Ghiorso, M., and Cutler, I. (2009) Structure, thermodynamic, and transport properties of $CaAl_2Si_2O_8$ liquid. Part I: Molecular dynamics simulations. American Mineralogist, 73, 6918–6936.

Sun, N., Stixrude, L., de Koker, N., and Karki, B.B. (2011) First principles molecular dynamical simulations of diopside ($CaMgSi_2O_6$) liquid to high pressure. Geochimica et Cosmochimica Acta, 75, 3792–3802.

Tinker, D., Lesher, C.E., and Hutcheon, I.D. (2003) Self-diffusion of Si and O in diopside-anorthite melt at high pressure. Geochimica et Cosmochimica Acta, 67, 133–142.

Tinker, D., Lesher, C.E., Baxter, G.M., Uchida, T., and Wang, Y. (2004) High-pressure viscometry of polymerized silicate melts and limitations of the Eyring equation. American Mineralogist, 89, 1701–1708.

Urbain, G., Bottinga, Y., and Richet, P. (1982) Viscosity of liquid silica, silicates, and alumino-silicates. Geochimica et Cosmochimica Acta, 46, 1061–1072.

MANUSCRIPT RECEIVED FEBRUARY 4, 2012
MANUSCRIPT ACCEPTED JULY 26, 2012
MANUSCRIPT HANDLED BY CHARLES LESHER